

INSTITUTE OF EXPERIMENTAL PHYSICS

INSTITUTE OF EXPERIMENTAL PHYSICS

SLOVAK ACADEMY OF SCIENCES



THE 21st SMALL TRIANGLE MEETING on theoretical physics



**THE 21st SMALL TRIANGLE MEETING
on theoretical physics**

ISBN 978-80-8143-280-4
EAN 9788081432804

October 6–9, 2019 | Spišské Tomášovce

SLOVAK ACADEMY OF SCIENCES

**INSTITUTE OF EXPERIMENTAL PHYSICS
SLOVAK ACADEMY OF SCIENCES**

THE 21st SMALL TRIANGLE MEETING
on theoretical physics

October 6–9, 2019

Spišské Tomášovce

The 21st Small Triangle Meeting on theoretical physics was supported by grant of Plenipotentiary of Slovak Republic in the Joint Institute for Nuclear Research in Dubna. This publication is the result of the project implementation: MODEX ITMS2014+ 313011T548 supported by the Operational Programme Integrated Infrastructure (OPII) funded by the ERDF and project MAGBBRIS EURONANOMED III.

Published by the Institute of Experimental Physics,
Watsonova 47, 040 01 Košice, Slovakia

Edited by J. Buša, M. Hnatič, and P. Kopčanský

All articles published in this proceedings were peer reviewed.

Copyright © M. Hnatič and P. Kopčanský, 2020

ISBN

PREFACE

This proceedings comprises the talks presented at the 21st *SMALL TRIANGLE MEETING on theoretical physics* conference, which was held in Spišské Tomášovce, Slovakia, on October 6–9, 2019. The STM conference is organized annually since 1999.

The aim of the conference is to serve as a forum for meeting between theoretical and experimental physicists especially from Ukraine, Russia, Finland, Hungary, Czech Republic, Poland and Slovakia, where scientists from different research areas of physics met together. This provides an ideal opportunity to exchange knowledge, ideas and experiences. We are convinced that it helps us in our work and that we will find joint tasks in the future scientific collaboration.

The scientific program presented at this year's meeting covered the research areas from solid state physics through nonlinear dynamical systems, atomic, nuclear, high energy physics to biophysics. The final program included 30 oral presentations. We would like to thank the authors for their cooperation and we are looking forward for the next STM meeting.

All articles published in this proceedings were peer reviewed.

Editors

Program Committee

Ján Buša, Laboratory of Information Technologies, JINR, Dubna, Russia
Michal Hnatič, Faculty of Science, P. J. Šafárik University, Košice
& Institute of Experimental Physics, SAS, Košice, Slovakia
& BLTP, Joint institute for Nuclear Research, Dubna, Russia
Juha Honkonen, National Defence University, Helsinki, Finland
Alexei Gladyshev, BLTP, Joint institute for Nuclear Research, Dubna, Russia
Volodymyr Lazur, Faculty of Physics, Uzhgorod National University, Ukraine
Peter Kopčanský, Institute of Experimental Physics, SAS, Košice, Slovakia

List of participants

Rafal Bielas, Adam Mickiewicz University of Poznań, Poland
Šarlota Birnšteinová, FNS UPJŠ, Košice, Slovakia
Sergii Burylov, Institute of Transport Systems and Technologies, NASU, Dnipro
Serge Bondarenko, BLTP, JINR, Dubna, Russian Federation
Alla Fershtynska, FLNP, JINR, Dubna, Russian Federation
Natalia Gavrilo, D. Mendeleev University of Chemical Technology, Moscow, Russia
Alexei Gladyshev, JINR, Dubna, Russian Federation
Vladimir Gorev, NRC Kurchatov Institute, Moscow, Russian Federation
Michal Hnatič, PJŠU & IEP SAS, Košice, Slovakia & BLTP JINR,
Slavomír Hnatič, IEP SAS, Košice, Slovakia & LIT JINR, Dubna, Russia
Gabriela Hnatičová, IEP SAS, Košice, Slovakia
Juha Honkonen, HU, Helsinki, Finland
Arkadiusz Jozefczak, Adam Mickiewicz University of Poznań, Poland
Katarzyna Kaczmarek, Adam Mickiewicz University of Poznań, Poland
Polina Kakin, SPbSU, Sankt Petersburg, Russian Federation
Georgii Kalagov, FNS P. J. Šafárik University, Košice, Slovakia
Mikhaylo Khoma, Uzhgorod National University, Uzhgorod, Ukraine
Nataliya Kondor, Uzhgorod National University, Uzhgorod, Ukraine
Peter Kopčanský, IEP SAS, Košice, Slovakia
Olexander Kovalchuk, IP, NASU, Kyiv, Ukraine
Sergey Kovalchuk, IP, NASU, Kyiv, Ukraine
Tatiana Kovalchuk, IP, NASU, Kyiv, Ukraine
Norbert Kučerka, FLNP JINR, Dubna, Russian Federation
Yuri Kulchitsky, LNP JINR, Dubna, Russia
Nikita Lebedev, BLTP, JINR, Dubna, Russian Federation
Vladimír Lisý, FEE&I TU, Slovakia & LRB JINR, Dubna, Russia
Tomáš Lučivjanský, FNS P. J. Šafárik University, Košice, Slovakia
Martin Menkyna, IEP SAS, Košice, Slovakia
Lukáš Mižišin, FNS P. J. Šafárik University, Košice, Slovakia
Ivan Nebola, UzhNU, Uzhgorod, Ukraine
Andrey Pikelner, BLTP, JINR, Dubna, Russian Federation
Olexander Reity, UzhNU, Uzhgorod, Ukraine
Richard Remecký, IEP SAS, Košice, Slovakia
Vasil Rubish, UzhNU, Uzhgorod, Ukraine
Ivo Šafárik, University of South Bohemia in České Budějovice, Czech Republic

Milan Timko, IEP SAS, Košice, Slovakia

Janka Tóthová, FEE&I TU, Košice, Slovakia

Alexei Uteshev, SPbSU, Sankt Petersburg, Russian Federation

Contents

Š. Birnštejnová, M. Hnatič, T. Lučivjanský: <i>Effect of long-range spreading on two-species reaction-diffusion system</i>	8
S.G. Bondarenko, V.V. Burov, S.A. Yurev: <i>Helium-3 charge form factor with relativistic rank-one separable kernel</i>	14
N.N. Gavrilova: <i>Knudsen diffusion conditions for intensification of catalytic reactions on membrane catalysts</i>	22
V.V. Gorev: <i>Free electron laser and the European XFEL project</i>	30
M. Hnatič, T. Lučivjanský, L. Mižišin: <i>Effects of turbulent mixing on the tricritical behavior of the directed percolation</i>	36
J. Honkonen: <i>Perturbation theory of degenerate boson gas</i>	44
E. Jurčišinová, M. Jurčišín, R. Remecký: <i>Anomalous scaling in the kinematic magnetohydrodynamic turbulence</i>	54
M.V. Khoma, V.Yu. Lazur, S.I. Myhalyna: <i>The comparative study of the post and the prior form of the electron capture amplitude in the Dodd-Greider formalism at intermediate and high collision energies</i>	62
T. Kondela, O.I. Ivankov, E.V. Ermakova, T.N. Murugova, D.R. Badreeva, E. Dushanov, K.T. Kholmurodov, A.I. Kuklin, N. Kučerka: <i>Interactions in the pre-AD mimicking model membraness</i>	72
N.Yu. Kondor, O.V. Yegiazarian, E.A. Nagy, S.V. Gedeon, V.F. Gedeon, V.Yu. Lazur: <i>Calculations of the energy structure of P, S atoms by the R-matrix method with B-splines</i>	82
P. Kopčanský, M. Timko, J. Kováč, O. Štrbák: <i>Focused magnet for magnetic drug targeting</i>	92
V.Yu. Lazur, V.V. Rubish, O.K. Reity, S.I. Myhalyna: <i>Description of mass spectrum of B_c-meson family</i>	98
V. Lisý, J. Tóthová: <i>Generalized Langevin equations and fluctuation-dissipation theorem for particle-bath systems in electric and magnetic fields</i>	108
M. Menkyna: <i>Finite time correlations in compressible Kraichnan model</i>	116
I.I. Nebola, A.F. Katanytsia, I.M. Shkyrta, J.M. Pozho: <i>Model calculations of phonon dispersion of complex crystals with partially populated crystallographic positions</i>	126
O.K. Reity, V.K. Reity, V.Yu. Lazur: <i>Quasiclassical theory of tunnel ionization of an atom by the perpendicular electric and magnetic fields</i>	136
A.V. Stadnik, P.S. Sazhin, S. Hnatic: <i>Construction of cascaded neural network classifiers and analysis of their effectiveness</i>	146
Photo Gallery	150

- [28] G. Pabst, N. Kučerka, M.P. Nieh, M.C. Rheinstädter, J. Katsaras, *Chem. Phys. Lipids* **163**, 460 (2010).
- [29] S. Dante, T. Hauss, N.A. Dencher, *Biophys. J.* **83**, 2610 (2002).
- [30] I. Ermilova, A.P. Lyubartsev, *RSC Adv.* **10**, 3902 (2020).
- [31] R.L. Sack, A.J. Lewy, D.L. Erb, W.M. Vollmer, C.M. Singer, *J. Pineal Res.* **3**, 379 (1986).



Calculations of the energy structure of **P**, **S** atoms by the *R*-matrix method with *B*-splines

N.Yu. Kondor, O.V. Yegiazarian, E.A. Nagy, S.V. Gedeon,
V.F. Gedeon, V.Yu. Lazur

*Department of Theoretical Physics, Uzhhorod National University,
Voloshina 54, 88000 Uzhhorod, Ukraine*

Abstract

The energy structure of phosphorus and sulfur atoms was calculated using the *R*-matrix method with *B*-splines (**BSR** method). This method provides a fairly complete account of the effects of valence and cor-valence electron correlation. Using the multiconfiguration Hartree-Fock method (**MCHF**), multiconfiguration calculations of the properties of the electronic structure of sulfur and phosphorus atoms were performed, which will later be used in the study of electron scattering processes on **P** and **S** atoms.

1 Introduction

In recent decades, there has been an intensive development of research on the processes of electron-atomic (**EA**) collisions. The importance of the results of systematic calculations of the structure properties of phosphorus and sulfur atoms for various applications in atomic physics, the theory of electron-atomic collisions and plasma modeling can not be overestimated. Thus, elementary processes involving atoms and ions play an important role in plasma injection and diagnostics in modern thermonuclear installations and affect the processes occurring in the plasma itself, determine the operating conditions of x-ray and gas lasers, and are important in the design and use of heavy ion accelerators.

In this paper, calculations of the energy structure of phosphorus and sulfur atoms were performed using the *R*-matrix method proposed in [1]–[9] with non-orthogonal orbitals and *B*-splines as basic functions (**BSR**) [10]. The multiconfiguration Hartree-Fock method (**MCHF**) [11] with non-orthogonal orbitals optimized in independent calculations for individual terms was also used in calculations of the energy structure of **P** and **S** atoms. The results obtained will be used in the future to study the processes of scattering of slow electrons on phosphorus and sulfur atoms.

2 Materials and methods

In this section, we will briefly consider the main aspects of the new version of the *R*-matrix method with *B*-splines (**BSR** method)[10]. This method is successfully used both in calculations of atomic structure and in the study of elastic and

inelastic scattering of slow electrons in complex atoms and ions. A special feature of the **BSR** method is the use of basic splines B_i to represent both the bound orbitals of the target atom and the orbitals of the scattered electron. The problem of low-energy electron scattering on an N -electron atom is reduced to solving the Schroedinger equation

$$(H_{N+1} - E) \Psi_\alpha^\Gamma(X, x_{N+1}) = 0, \quad (1)$$

$$H_{N+1} = \sum_{i=1}^{N+1} \left(-\frac{1}{2} \nabla_i^2 - \frac{Z}{r_i} \right) + \sum_{i>j=1}^{N+1} \frac{1}{r_{ij}}$$

with the appropriate limit conditions. Here E and H_{N+1} are the total energy and the Hamiltonian $H_{(N+1)}$ - of the electron system "atom + solid electron", Z is the charge of the nucleus. The Hamiltonian $H_{N+1}(1)$ is diagonal with respect to the total orbital moment L , the total spin S , their projections M_L, M_S on a given axis, and the parity π . The function $\Psi_\alpha^\Gamma(X, x_{N+1})$, which is usually called the collision wave function, is a completely antisymmetrized wave function $(N+1)$ of an electron system, $X \equiv (x_1, \dots, x_N)$, $\Gamma \equiv (\gamma L S M_L M_S \pi)$, and denotes the set of spatial \vec{r}_i and spin σ_i coordinates of the i -th electron. The index α characterizes the initial conditions and usually denotes the input channel of $e+A$ scattering. Without taking into account ionization the schedule of the full contact wave function $\Psi_\alpha^\Gamma(X, x_{N+1})$ can be presented as:

$$\Psi_\alpha^\Gamma(X, x_{N+1}) = A \sum_{i=1}^n \bar{\Phi}_i^\Gamma(X; \hat{r}_{N+1}, \sigma_{N+1}) \frac{F_{i\alpha}^\Gamma(r_{N+1})}{r_{N+1}} + \sum_{j=1}^m c_j \chi_j^\Gamma(X, x_{N+1}). \quad (2)$$

Here \mathbf{A} is the anti-symmetry operator; $\bar{\Phi}_i^\Gamma$ - the wave function of the i -th channel, which is constructed by vector coupling of the wave function of the N -electron target $\Phi_i(X)$ with the angular and spin parts of the wave function of the scattered electron; $\chi_j^\Gamma(X, x_{N+1})$ - a set of quadratically-integrable anti-symmetric correlation functions that ensure the completeness of the decomposition (2). The problem is to find the radial wave functions $F_{i\alpha}^\Gamma(r_{N+1})$ of the scattered electron and the coefficients $c_j(2)$. The atomic wave functions of $\Phi_i(X)$ are constructed in the form of a multi-configuration schedule:

$$\Phi_i(x_1, \dots, x_N) = \sum_j c_{ij} \varphi_j(x_1, \dots, x_N), \quad (3)$$

where φ_j - one-dimensional wave functions of the target atom. The c_{ij} coefficients are obtained by diagonalizing the N -electron Hamiltonian H_N of the target atom:

$$\langle \Phi_i | H_N | \Phi_j \rangle = E_i(Z, N) \delta_{ij}. \quad (4)$$

Usually, the first sum in the right part of the decomposition (2) includes only those target states that at a given energy $E = E_i + \frac{k^2}{2}$ correspond to the so-called open channels. The first sum can also include some pseudo-states that approximate the States of a continuous spectrum. The choice of pseudo-stations

is based on the exact account of the polarizability of the main and several excited states of the target. In addition to using pseudo-stations, the contribution of closed channels can be partially accounted for using a finite number of correlation functions $\chi_j^\Gamma(X, x_{N+1})$, included in the second sum of the expansion (2).

The basic functions φ_j and χ_j in the layouts (2), (3) are constructed from single-electron atomic orbitals φ_{α_i} , which in the central field approximation have the form:

$$\varphi_{\alpha_i}(x) = 1/r \cdot P_{n_i l_i}(r) Y_{l_i m_i}(\hat{r}) \chi(m_s | \sigma), x \equiv (\vec{r}_i', \sigma), \quad (5)$$

where α_i is the abbreviation for the set of quantum numbers n_i , l_i , m_i and m_s . In the standard \mathbf{R} -matrix approach, for convenience of calculations, the radial wave functions of the scattered electron $F_{i\alpha}^\Gamma$ are chosen orthogonal to all the atomic orbitals of the target $P_{n_j l_j}$ of the same symmetry, i.e.

$$\int_0^\infty P_{n_j l_j}(r) F_{i\alpha}^\Gamma(r) dr = 0 \quad (6)$$

where $l_j = l_i$. Condition (4) actually means that the incoming electron cannot be virtually captured in one of the empty sub-columns included in the schedule (3) of target states.

Substituting the expansion (2) in equation (1), multiplying it alternately by functions $\overline{\Phi}_i^\Gamma$ and χ_j^Γ , we obtain after integration over all variables except r_{N+1} , a system of integro-differential equations for functions $F_i \equiv F_{i\alpha}^\Gamma$:

$$\left(\frac{d^2}{dr^2} - \frac{l_i(l_i + 1)}{r^2} + \frac{2Z}{r} + k_i^2 \right) F_i(r) = 2 \sum_j (V_{ij} + W_{ij} + X_{ij}) F_j(r), \quad (7)$$

anywhere $k_i^2 = 2[E - E_i(Z, N)]$, and V_{ij} , W_{ij} , X_{ij} are the local direct, non-local exchange and non-local correlation potentials, respectively. For electron scattering in complex atoms, the explicit form of these potentials is generated automatically by the **BSR** program [10], depending on the type of input data.

A variant of the \mathbf{R} -matrix method, which is based on the use of non-orthogonal orbitals and \mathbf{B} -splines as basic functions, is applied to the solution of the system of equations of **SC**(5). This method allows us to describe various types of reactions, such as elastic scattering, excitation and ionization of an atom by an electron shock, within a single formalism. The main idea of the \mathbf{R} -matrix method is to divide the configuration space of the atom + electron system into two regions: internal $\mathbf{r} < \mathbf{a}$ and external $\mathbf{r} > \mathbf{a}$. The radius of the inner region $\mathbf{r} = \mathbf{a}$ is chosen so that the exchange and correlation effects are small enough for $r \geq a$. The complete wave function ($\mathbf{N}+1$) of an electronic system in the inner region can be represented at a given energy \mathbf{E} as an expansion:

$$\Psi_E^\Gamma = \sum_k A_{Ek}^\Gamma \Psi_k^\Gamma \quad (8)$$

independent on the energy of a discrete basis set Ψ_k^Γ :

$$\Psi_k^\Gamma(X, x_{N+1}) = A \sum_{ij} \bar{\Phi}_i^\Gamma(X; \hat{r}_{N+1}, \sigma_{N+1}) \frac{u_j(r_{N+1})}{r_{N+1}} c_{ijk}^\Gamma + \sum \chi_i^\Gamma(X, x_{N+1}) d_{ik}^\Gamma, \quad (9)$$

where $\bar{\Phi}_i^\Gamma$ and χ_i^Γ are defined in the same way as in formula (2). We present the functions $F_{i\alpha}^\Gamma$ describing the radial motion of a scattered electron in the i -th channel as a linear combination of a finite number of basic functions u_j satisfying the boundary conditions: $u_j = 0$, $(a/u_j)du_j/dr|_{r=a} = b$ where b is an arbitrary real constant. For such basic functions, the Hamiltonian (1) in the inner domain is not hermitian due to non-zero (for $r = a$) surface terms arising from the kinetic energy operator. However, these members can be deleted using the Bloch operator L_{N+1} . The formal solution of the Schrodinger equation (1) takes the form:

$$|\Psi\rangle = \frac{1}{2} \sum_{kj} |\Psi_k^\Gamma\rangle \langle \bar{\Phi}_j^\Gamma | (E_k - E)^{-1} \left(\frac{d}{dr_{N+1}} - \frac{b_j}{r_{N+1}} \right) \langle \bar{\Phi}_j^\Gamma | \Psi \rangle. \quad (10)$$

By projecting this equation on channel functions $\bar{\Phi}_i^\Gamma$ and performing calculations on the boundary of the inner region, we get

$$F_i^\Gamma(a) = \sum_{j=1}^n R_{ij}^\Gamma(E) \left(\frac{adF_j^\Gamma}{dr_{N+1}} - b_j F_j^\Gamma \right)_{r_{N+1}=a}, \quad (11)$$

where we introduced an \mathbf{R} -matrix with elements

$$R_{ij}^\Gamma(E) = \frac{1}{2a} \sum_k \frac{w_{ik}^\Gamma(a) w_{jk}^\Gamma(a)}{(E_k^\Gamma - E)}, \quad (12)$$

radial functions F_i^Γ and surface amplitudes w_{ik}^Γ are given. Diagonalizing matrix $\langle \Psi_k^\Gamma | H_{N+1} + L_{N+1} | \Psi_k^\Gamma \rangle_{int}$ for each set of quantum numbers Γ , we can determine the energy E_k^Γ and the coefficients c_{ijk}^Γ , d_{ik}^Γ in schedule (7), that is, wave functions Ψ_k^Γ for the corresponding base states. However, this only needs to be done once to determine the \mathbf{R} -matrix over the entire range of collision energies.

As noted above, the inclusion of additional correlation functions χ_j^Γ in the output schedule (7) allows us to partially account for the effects associated with the orthogonality conditions of (4) functions $F_{i\alpha}^\Gamma$ and the restriction of the first sum in (7) to a finite number of summands. However, this leads in most cases to the appearance of a pseudo-resonant structure in the scattering cross sections and to an excessively large number of additional integro-differential equations, which must be left in (7) for realistic calculations of complex atoms and their interaction with electrons. In this regard, we note that condition (4) is not mandatory and does not follow from general quantum mechanical principles. Therefore, in our papers [1]–[9], we abandoned the requirement (4) for orthogonality of functions $F_{i\alpha}^\Gamma(r_{N+1})$ connected to the target orbital $P_{n_j} l_j$ of the same symmetry. We also note that in the proposed **BSR** version of the R -matrix method, we can do without

any correlation functions χ_j^Γ , or use them only to compensate for defects in the collision function, associated with limiting the first sum in the (7) scenario to a finite number of terms.

3 Results and discussion

A) The energy structure of the P atom. The structure calculations for the P atom were performed using both the **MCHF** package [11], and the **BSR** package [10]. Using the **BSR** method, single-electron orbitals of **39** lower states of the **P** atom with configurations $1s^2 2s^2 2p^6 3s^2 3p^3 ({}^4S^o, {}^2D^o, {}^2P^o)$, $3s^2 3p^2 ({}^3P) nl$ ($n = 3, 4, 5, 6; l = 0, 1, 2$), $3s^2 3p^2 ({}^1D) nl$ ($n = 4; l = 0, 1$), $3s^2 3p^2 ({}^1P) 4s$ and $3s 3p^4 ({}^4P, {}^2D, {}^2S)$, in the **LS**-approximation. The spectrum of the phosphorus atom according to **NIST** data [12] is quite complex. The next several levels of the spectrum **P** are formed primarily by exciting a single $3p$ electron from the valence shell at some of the spectroscopic levels of the $3s^2 3p^2 ({}^3P) nl$ ($n = 3, 4, 5, 6, 7; l = 0, 1, 2, 3, 4$) configuration. However, the 6th **LS**-level $3s 3p^4 {}^4P$ is formed by the excitation of the $3s$ electron, as a result, we have to consider configurations with vacancies in the inner $3s$ shell. The 8th **LS**-level $3s^2 3p^2 ({}^1D) 4s {}^2D$, formed with an intermediate 1D -, rather than 3P - term, as in other cases, also causes difficulties. All this requires significant adjustments to the scheme for calculating the configuration states of the phosphorus atom. The presence in the lower part of the spectrum of states with a frozen $3s$ shell indicates the need to take into account not only the valence, but also the cor-valence correlation in the calculations. The relatively small charge of the nucleus and the absence of strong splitting of levels at the **LSJ** sublevel indicate a relatively insignificant role of relativistic effects in the calculations of the lowest energy levels of the **P** atom.

Fig.1 shows the results of calculating the energies of the **39** lower levels of the **P** atom. The main attention is paid to obtaining the exact excitation energies of spectroscopic States under the first ionization threshold and taking into account the microelectron correlation when calculating the corresponding wave functions. To control the accuracy of calculating the wave functions of the atom **P**, the forces of oscillators between the main one - and two-electron transitions are also calculated. The multi-configuration Hartree-Fock (**MCHF**) excitation energies calculated by us are compared with the reference data of **NIST**[12].

Fig.1 shows that in the case of a phosphorus atom, the standard procedure for calculating the energies of spectroscopic States using orbitals that are orthogonalized in independent calculations for individual terms is very difficult. For example, for term 4P , it is necessary to calculate single-electron orbitals of configurations $3s^2 3p^2 ({}^3P) 4s; 3s 3p^4; 3s^2 3p^2 ({}^3P) 5s, 3d, 4d, 6s$ with two different atomic residues $3s^2 3p^2 ({}^3P)$ and $3s 3p^4$. This determines the need to take into account two different $3p$ orbitals of the atomic phosphorus residue for this term in further calculations. For **Fig.2** we compared the calculated **BSR** excitation energies of E_{BSR} with the reference data of **NIST** (E_{NIST}). The resulting accuracy of the **BSR** energies is mainly in the range of $\sim 0.05 - 0.2$ eV, which makes it possible to use them to calculate electron scattering processes on the **P** atom. As can be seen from **Fig.2**, the phosphorus atom is characterized by a fairly high ionization threshold E_{ion}

No	Conf	Term	E_{ex} NIST	E_{ex} MCHF	ΔE_{ex}
1	$3s^2 3p^3$	$^4S^o$	0.0	0.0	0.0
2	$3s^2 3p^3$	$^2D^o$	1.410	1.426	-0.016
3	$3s^2 3p^3$	$^2P^o$	2.323	2.294	0.030
4	$3s^2 3p^2(^3P)4s$	4P	5.971	6.249	-0.278
5	$3s^2 3p^2(^3P)4s$	2P	7.200	7.178	0.023
6	$3s^2 3p^4$	4P	7.395	6.540	0.855
7	$3s^2 3p^2(^3P)4p$	$^2S^o$	7.965	8.008	-0.043
8	$3s^2 3p^2(^1D)4s$	2D	8.078	8.337	0.259
9	$3s^2 3p^2(^3P)4p$	$^4D^o$	8.136	8.146	-0.011
10	$3s^2 3p^2(^3P)4p$	$^4P^o$	8.239	8.198	0.041
11	$3s^2 3p^2(^3P)4p$	$^2D^o$	8.306	8.801	-0.495
12	$3s^2 3p^2(^3P)4p$	$^4S^o$	8.286	8.383	-0.096
13	$3s^2 3p^2(^3P)3d$	2P	8.429	8.727	-0.298
14	$3s^2 3p^2(^3P)4p$	$^2P^o$	8.437	8.338	0.099
15	$3s^2 3p^2(^3P)3d$	4F	8.478	8.557	-0.079
16	$3s^2 3p^2(^3P)3d$	4D	8.671	8.669	0.002
17	$3s^2 3p^2(^3P)3d$	2F	8.749	8.763	-0.015
18	$3s3p^4$	2D	8.825	9.68	-0.858
19	$3s^2 3p^2(^3P)5s$	4P	9.008	9.015	-0.006
20	$3s^2 3p^2(^3P)3d$	4P	8.984	8.057	0.927
21	$3s^2 3p^2(^3P)3d$	2D	9.029	8.933	0.096
22	$3s^2 3p^2(^3P)5s$	2P	9.069	8.980	0.089
23	$3s^2 3p^2(^1D)4p$	$^2D^o$	9.211	9.349	-0.138
24	$3s^2 3p^2(^1D)4p$	$^2F^o$	9.265	9.265	0.000
25	$3s^2 3p^2(^3P)5p$	$^2S^o$	9.312	9.242	0.069
26	$3s^2 3p^2(^3P)5p$	$^4D^o$	9.364	9.286	0.078
27	$3s^2 3p^2(^1D)4p$	$^2P^o$	9.358	9.547	-0.189
28	$3s^2 3p^2(^3P)4d$	2P	9.393	9.439	0.046
29	$3s^2 3p^2(^3P)5p$	$^4P^o$	9.398	9.298	0.10
30	$3s^2 3p^2(^3P)4d$	2F	9.411	9.464	-0.053
31	$3s^2 3p^2(^3P)4d$	4F	9.443	9.404	0.040
32	$3s^2 3p^2(^3P)5p$	$^4S^o$	9.425	9.370	0.055
33	$3s^2 3p^2(^3P)5p$	$^2D^o$	9.464	9.378	0.086
34	$3s^2 3p^2(^3P)4d$	4D	9.503	9.418	0.085
35	$3s^2 3p^2(^3P)5p$	$^2P^o$	9.527	9.273	0.253
36	$3s^2 3p^2(^1S)4s$	2S	9.536	9.664	0.128

Figure 1: The excitation energies (in eV) of the phosphorus atom: our **MCHF** calculations of the excitation energies are compared with **NIST** data [12].

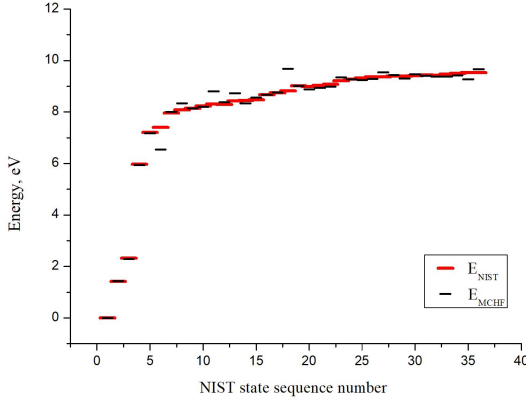


Figure 2: Scheme of placement of energy thresholds of excitation of the phosphorus atom. The data of our **BSR** calculations (E_{BSR}) is comparable to the data of NIST (E_{NIST})

= 10.49 eV. However, there is too narrow an energy interval between the main $3p^3\ ^4S^o$ -state and the lower excited states of the same configuration $3p^3\ ^2D^o$ and $3p^3\ ^2P^o$. In this case, the excitation energy of the above States is 0.0; 1.4097 and 2.3234 eV, respectively.

B) The energy structure of the S atom.

Using the program code **MCHF**, we calculated **38** lower states of the **S** atom with configurations $1s^22s^22p^63s^23p^4\ (^3P, ^1D, ^1S)$, $3s^23p^3\ (^4S^o)nl$ ($n = 3, 4, 5, 6; l = 0, 1, 2$), $3s^23p^3\ (^2D^o)nl$ ($n = 4; l = 0, 1$), $3s^23p^3\ (^2P^o)4s$ and $3s3p^5\ (^3, ^1P^o)$. As in the case of the phosphorus atom, the spectrum of the sulfur atom, according to **NIST** [13], cannot be attributed to simple ones. As can be seen from Fig.3, the sulfur atom is characterized by a fairly high ionization threshold $E_{ion} = 10.36$ eV. The three lower levels ($^3P, ^1D, ^1S$) correspond to the $3s^23p^4$ ground state configuration with energies of **0.02427**, **1.1454**, and **2.7500** eV, respectively. The value of the ground state energy is obtained by weight averaging the levels of the $3s^23p^4\ ^3P_{0,1,2}$ triplet fine structure during the transition from the LSJ-NIST image to the **LS**-link approximation used by us. The next several levels of the spectrum of the **S** atom are formed primarily by exciting a single $3p$ electron from the valence shell at some of the spectroscopic levels of the $3s^23p^3\ (^4S^o)nl$ ($n = 3, 4, 5, 6, 7; l = 0, 1, 2, 3, 4$) configurations. However, already the 9th and 11th in order **LS**-level $3s^23p^3\ (^2D)4s\ ^3, ^1D$ are formed with an intermediate 2D -, not $^4S^o$ term. Even more difficult to calculate is the 15th **LS**-level $3s3p^5\ ^3P^o$ with a defrosted $3s$ shell. The presence in the lower part of the spectrum of the **S** atom of states with a $3s$ -frosted shell indicates the need to take into account not only the valence, but also the cor-valence correlation in the calculations. In addition, the presence of a stable negative sulfur ion S^- with a configuration of $3p^5\ P_{3/2}$ and an affinity energy of **2.0771** eV indicates the need to take into account the valence and cortical correlation in the calculations of $e+S$ scattering processes.

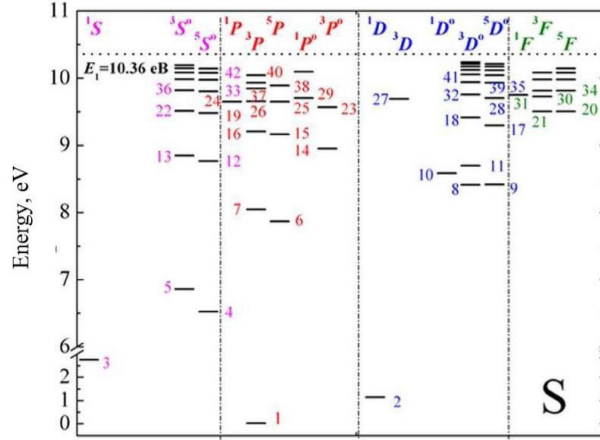


Figure 3: Layout of the 42 lower energy levels (*LS*-showing) of the sulfur atom and their distribution by termiae according to NIST data [13].

Fig.4 shows a comparison of multi-configuration Hartree-Fock (MCHF) excitation energies of E_{MCHF} with reference data from NIST [13] (E_{NIST}). The accuracy of the obtained MCHF-excitation energies of the states of the S atom is $\sim 0.04 - 0.2$ eV. When calculating wave functions and excitation energies, the main attention is paid to taking into account the effects of valence and cor-valence correlation. To control the accuracy of the calculated wave functions of the S atom, the oscillator forces for single- and double-electron transitions are calculated.

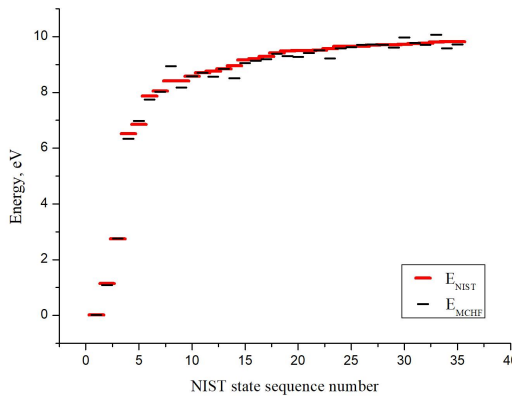


Figure 4: Layout of the energy thresholds of the E_{exit} excitation of the sulfur atom. The results of our MCHF calculations are compared with NIST data [13].

The numerical values of the excitation energies obtained by us in MCHF calculations are shown in Fig.5. The results of our calculations are in good agreement with the data from the NIST database [13].

No	Conf	Term	E_{ex} NIST	E_{ex} MCHF	ΔE_{ex}
1	$3s^23p^4$	3P	0.024	0.024	0.0
2	$3s^23p^4$	1D	1.145	1.089	0.057
3	$3s^23p^4$	1S	2.750	2.765	-0.015
4	$3s^23p^3(^4S^o)4s$	$^5S^o$	6.524	6.337	0.187
5	$3s^23p^3(^4S^o)4s$	$^3S^o$	6.860	6.974	-0.114
6	$3s^23p^3(^4S^o)4p$	5P	7.868	7.744	0.124
7	$3s^23p^3(^4S^o)4p$	3P	8.045	8.020	0.026
8	$3s^23p^3(^2D^o)4s$	$^3D^o$	8.410	8.940	-0.530
9	$3s^23p^3(^4S^o)3d$	$^5D^o$	8.417	8.171	0.246
10	$3s^23p^3(^2D^o)4s$	$^1D^o$	8.584	8.575	0.010
11	$3s^23p^3(^4S^o)3d$	$^3D^o$	8.700	8.705	-0.005
12	$3s^23p^3(^4S^o)5s$	$^5S^o$	8.766	8.569	0.197
13	$3s^23p^3(^4S^o)5s$	$^3S^o$	8.846	8.839	0.008
14	$3s3p^5$	$^3P^o$	8.952	8.508	0.444
15	$3s^23p^3(^4S^o)5p$	5P	9.165	9.059	0.106
16	$3s^23p^3(^4S^o)5p$	3P	9.208	9.131	0.077
17	$3s^23p^3(^4S^o)4d$	$^5D^o$	9.296	9.188	0.108
18	$3s^23p^3(^4S^o)4d$	$^3D^o$	9.417	9.393	0.024
19	$3s^23p^3(^4S^o)6s$	$^5S^o$	9.480	9.298	0.183
20	$3s^23p^3(^4S^o)4f$	5F	9.504	9.276	0.228
21	$3s^23p^3(^4S^o)4f$	3F	9.504	9.421	0.083
22	$3s^23p^3(^4S^o)6s$	$^3S^o$	9.512	9.514	-0.002
23	$3s^23p^3(^2P^o)4s$	$^3P^o$	9.567	9.222	0.345
24	$3s^23p^3(^4S^o)6p$	5P	9.653	9.583	0.069
25	$3s^23p^3(^2D^o)4p$	1P	9.653	9.627	0.026
26	$3s^23p^3(^4S^o)6p$	3P	9.658	9.708	-0.049
27	$3s^23p^3(^2D^o)4p$	3D	9.693	9.727	-0.034
28	$3s^23p^3(^4S^o)5d$	$^5D^o$	9.704	9.714	-0.010
29	$3s^23p^3(^2P^o)4s$	$^1P^o$	9.707	9.611	0.096
30	$3s^23p^3(^2D^o)4p$	3F	9.725	9.970	-0.245
31	$3s^23p^3(^2D^o)4p$	1F	9.750	9.770	-0.020
32	$3s^23p^3(^4S^o)5d$	$^3D^o$	9.757	9.704	0.052
33	$3s^23p^3(^4S^o)7s$	$^5S^o$	9.802	10.073	-0.271
34	$3s^23p^3(^4S^o)5f$	5F	9.812	9.583	0.230
35	$3s^23p^3(^4S^o)5f$	3F	9.813	9.726	0.086

Figure 5: The excitation energy (in eV) of the sulfur atom [13].

Summary

The comparison of the calculated excitation energies with the available experimental data indicates the high efficiency and accuracy of the **BSR** version of the **R**-matrix method proposed in our works [1]–[9], based on the use of non-orthogonal orbitals and **B**-splines as basic functions. The achieved accuracy is **0.05–0.2 eV** for lower energy levels, and we can assume that the electronic wave functions calculated by us take into account the effects of electronic correlations quite fully. The calculated values of the excitation energies and wave functions of the **39** lowest states of the **P** atom and the **38** lowest states of the **S** atom will be used in

the future to calculate the total and differential cross sections of the scattering of slow electrons on phosphorus and sulfur atoms.

Acknowledgments. In conclusion the authors wish to express their sincere gratitude to O. Zatsarinny and K. Bartschat for close cooperation and support in the work.

References

- [1] O. Zatsarinny, K. Bartschat, S. Gedeon, V. Gedeon, V. Lazur, *Phys. Rev. A.* **74**, 052708 (2006).
- [2] O. Zatsarinny, K. Bartschat, L. Bandurina, S. Gedeon, *J. Phys. B.* **40**, 4023 (2007).
- [3] O. Zatsarinny, K. Bartschat, S. Gedeon, V. Gedeon, V. Lazur, E. Nagy, *Phys. Rev. A.* **79**, 052709 (2009).
- [4] E.A. Nagy, *Uzhhorod Univ. Scient. Herald. Series. Phys.* **25**, 148 (2009).
- [5] V. Gedeon, S. Gedeon, V. Lazur, E. Nagy, O. Zatsarinny, K. Bartschat, *Phys. Rev. A.* **85**, 022711 (2012).
- [6] V. Gedeon, S. Gedeon, V. Lazur, E. Nagy, O. Zatsarinny, K. Bartschat, *Phys. Rev. A.* **92**, 052701 (2015).
- [7] V. Gedeon, S. Gedeon, V. Lazur, E. Nagy, O. Zatsarinny, K. Bartschat, *J. Phys. B.* **51**, 035004 (2018).
- [8] L.O. Bandurina, S.V. Gedeon, *Uzhhorod Univ. Scient. Herald. Series. Phys.* **37**, 49 (2015).
- [9] E.A. Nagy, V.F. Gedeon, S.V. Gedeon, V.Yu. Lazur, *Ukr. Phys. Journ.* **63**, 10 (2018).
- [10] O. Zatsarinny, *Comput. Phys. Commun.* **174**, 273 (2006).
- [11] C. Froese Fischer, *Comput. Phys. Commun.* **64**, 369 (1991).
- [12] A. Kramida, Yu. Ralchenko, J. Reader, and NIST ASD Team, *NIST Atomic Spectra Database* version 5.6.1, (2019), (<https://physics.nist.gov/asd>).
- [13] A. Kramida, Yu. Ralchenko, J. Reader, and NIST ASD Team, *NIST Atomic Spectra Database* version 4.1.0, (2019), (<https://physics.nist.gov/asd>).